Journal of Medicinal and Chemical Sciences 6 (2023) 986-999

Journal of Medicinal and Chemical Sciences

Journal homepage: http://www.jmchemsci.com/

Original Article

Effect of Yttrium Addition on Mechanical and Physical Properties of Ti15Mo Alloy as an Implant Materia

Yas Mohammed Musadaq[1]*, Ghassan Abdul-Hamid Naji[2,3], Haydar H. J. Jamal Al- Deen[4]

[1]*Department of Prosthodontics, College of Dentistry, University of Baghdad, Bab-Almoadham, P.O. Box 1417, Baghdad, Iraq*
[2]*College of Dentistry, University of Baghdad, Baghdad, Iraq*
[3]*Dean of College of Dentistry, The Iraqia University, Baghdad, Iraq*
[4]*Department of Metallurgical Engineering, Materials Engineering Faculty, University of Babylon, Hillah, Iraq*

ARTICLE INFO

Article history

Receive: 2022-07-26
Received in revised: 2022-08-14
Accepted: 2022-10-20
Manuscript ID: JMCS-2209-1766
Checked for Plagiarism: **Yes**
Language Editor:
Dr. Fatimah Ramezani
Editor who approved publication:
Dr. Yasser Fakri Mustafa

DOI:10.26655/JMCHEMSCI.2023.5.6

KEYWORDS

β-Titanium
Yttrium
Biomedical material
Powder metallurgy
Mechanical properties
Acid

ABSTRACT

The unique biomaterial multi-component Ti-Mo-xY (x = 0.5, 1.0, 1.5 wt. percent) alloys were created as a way to improve the mechanical characteristics and lessen the biomaterials' toxicity for implants to create new biomaterials for implant applications. This study aims to look at how adding yttrium (Y) changes the alloy's microstructure and mechanical characteristics. Through the use of powder metallurgy, Ti-Mo-xY (x = 0.5, 1.0, and 1.5 wt. percent) alloys are created. Atmospheric pressure high-purity argon gas is used to sinter the metals. The Brinell hardness tester was used for the hardness test, and optical, scanning, and scanning electron microscopes were used to characterize the microstructure. Ti-Mo-xY (x = 0.5, 1.0, 1.5 wt. percent) alloys tested hardness at 405.33, 435.76, and 510.05 HB, respectively. Ti-Mo-xY alloys with the enhanced compressive strength had values of 17.82, 18.04, and 18.14 MPa (where x = 0.5, 1.0, or 1.5 weight percent). The yttrium addition can significantly improve the mechanical properties of powder-metallurgical Ti alloys. Its cause may be related to the removed oxygen from the matrix and the strengthening action of Y oxides.

GRAPHICAL ABSTRACT

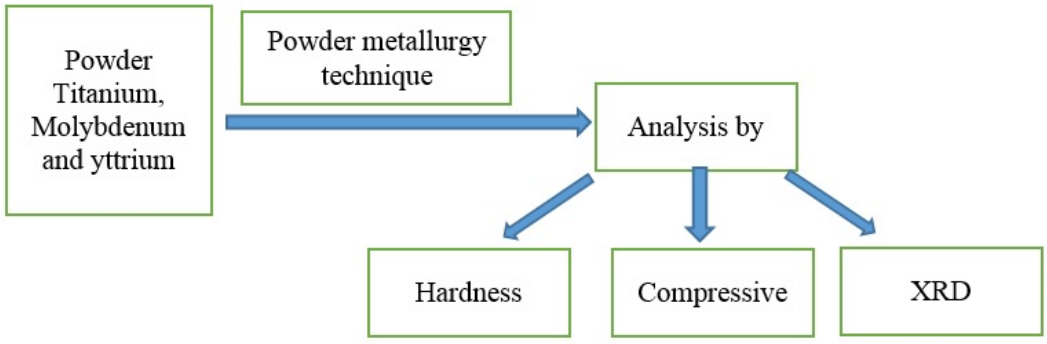

* Corresponding author: Yas Mohammed Musadaq
✉ E-mail: Email: yassalshahiab@gmail.com

Introduction

One of the most important scientific advances in clinical dentistry 40 years ago was the creation of Osseo integrated implants [1]. Because of their distinctive qualities, including corrosion resistance, biocompatibility, low density, and high modulus of elasticity, titanium, and its alloys have been employed in dentistry as supports and retainers for prosthetic equipment since the 1980s [2]. Due to titanium and its alloys' significantly higher elastic moduli and strength compared with human bones, stress shielding and implant failure might occur. E = 10–16 GPa is the titanium elasticity modulus, which is 8-10 times larger than bone [3]. To reduce the implants' modulus to a level comparable to that of human bones, researchers have tried to create new types of titanium alloys. On the other hand, the pore fraction and form of titanium can change its mechanical properties, and the stress-shielding effect is reduced. The porous titanium with a wide range of porosity can be produced using powder metallurgical procedures [4]. At low temperatures, Ti exhibits two allotropic states in thermodynamic equilibrium; at low temperatures, it has a compact hexagonal close packing (HCP), which is referred to as the matrix phase, while above 883°C, it does have a body-centered cubic structure (BCC) referred to as the transition temperature from pure titanium to pure titanium [5]. Most additional elements work to stabilize one phase or the other. Examples of α-stabilizers include Al, O, N, and C. In contrast, two types of β-stabilizers, isomorphous and -eutectoid have as their principal components, respectively, Mo, V, Y, Nb, and Ta, as well as Fe, W, Cr, Si, Ni, Co, Mn, and H. If properly treated, *β*-Isomorphous Ti alloys of implant have recently attracted interest due to the practical small elastic modules made with these metals. Some Ti alloys contain the "neutral" elements Zr and Sn, which are not thought to affect phase stability [6]. The equilibrium between the existing phases and interstitial element diffusion has a significant impact on the mechanical characteristics of titanium alloys [7]. The most significant benefit of β alloys over the other titanium alloys is their superior hardenability. They can be easily aged and solubilized, unlike β and α alloy to produce uniform precipitation [8]. The phase transitions that occur during heating and cooling as a result of the two allotropic titanium forms provide the basis for the heat treatment of titanium alloys. It is feasible to create desired structural modifications, which would subsequently modify their properties [9]. CPT and its alloys, primarily cobalt-based alloys and Ti-6Al-7Nb, Ti-6Al-4V, Co-Ni-Cr-Mo, Co-Cr-Mo, stainless steels (ABNT 316L steel), and noble alloys based on gold are the principal alloys utilized in biomedical applications. Due to the toxicity level seen in alloys including vanadium and aluminum (associated with neurological diseases in their composition), titanium alloys for biomedical purposes have been produced without these toxic elements, using materials such as niobium, tantalum, zirconium, molybdenum, and iron [10]. That led to alloys such as Ti–13Nb–13Zr, Ti–29Nb–13Ta–4,6Zr [11], Ti–15Mo [12], and Ti-Y [13]. The elastic modulus mismatch between biomaterials and surrounding bones is the key reason for the successful fixation of implantation materials to bone tissue remains a challenge. However, for the embedded materials to function for a considerably longer time, or perhaps for a lifetime without loss or revision surgery, they should be strong and resilient enough to withstand the physiological demands imparted. An effective balance between rigidity and strength is also required to complement the bone. Porous materials have been introduced to further lower the elastic modulus of alloys based on titanium. The elastic modulus is a quality that is difficult to change, as we are all aware. In addition, in the current work, targeted elements can be added to change the elastic modulus. Otherwise, porosity in the alloys used to create the final product determines the elastic modulus [14]. Numerous experiments are conducted to make Ti alloys containing yttrium. Ti alloys containing yttrium are biocompatible [12]. The recent studies have focused on β-type alloys minimizing the stress-shielding effect by having low elastic moduli. These alloys are created using stabilizers and non-cytotoxic materials such as molybdenum, tantalum, niobium, zirconium,

yttrium, and manganese indium [12-17]. Modern alloys have an elasticity modulus that is three to four times greater than that of human bone, which can be uncomfortable for the patient and increase the risk of implant failure. This is due to a condition called stress shielding [18], in which the implant's heavy mechanical strain causes degradation and decreased bone density, leaving the bones exposed. The therapeutic effectiveness of dental implants is improved by the yttrium addition to Ti due to improvements in biocompatibility, mechanical characteristics, and corrosion resistance [19].

It has been attempted to do an experimental study on Ti-15Mo-xY alloys. The literature lacks sufficient information on how mechanical properties and stages relate to one another. Therefore, a thorough structural analysis of this process is required to ensure a thorough grasp of the mechanical properties. The goal of the current work is to create a low-modulus β- type Ti-Mo alloy and examine its microstructure and mechanical properties following the yttrium addition to suggest it as a substitute material for biomedical applications.

Experimental procedure

In this investigation, the powdered forms of the elements (titanium, molybdenum, and yttrium) were used, all of which were obtained from Lemandou Ltd. Co. China. Table 1 presents the results of particle size analyzer (Nano-Brook 90Plus) and X-ray fluorescence (XRF) (Bruker S8 Tiger) tests performed on the starting materials to determine their purity.

Table 1: The purity and the average particle size of the used powders

Powder	Purity	Average particles size (μm)
Titanium	99.95	28.62
Molybdenum	99.98	23.59
Yttrium	99.99	19.43

Preparation of sample

Powder metallurgy was used to create Ti-15Mo-xY alloy and titanium alloy preforms. Alloys were fabricated via powder metallurgy, which entails three main processes: blending, cold compaction, and sintering. The powders of Ti-15Mo and xY were mixed in a ball mill for 8 hours.

The reinforcing particles were blended into the matrix phase to lessen the heterogeneous effects of the alloy. To make green preforms, cold compression was performed using the necessary quantity of mixed powder. Balls and powder are mixed at a weight ratio of 20:1 and a speed of 300 revolutions per minute. The powder was compacted using the punch and die. The powder was carefully measured and placed in the hollow die, and then the punch was set on top. By applying a known pressure of 850 MPa for 3 minutes at a constant loading rate (0.3 t/s) in a 100-ton hydraulic press, a green compact of varying dimensions was formed [20].

Graphite powder was sprinkled on both the inside and outside of the die and punched to act as a lubricant during the compacting process [19]. One of the main functions of this lubricant is to reduce the amount of wear and tear on the punch and die caused by the powder particles' contact with them. The green compacts were easily released from the die thanks to this lubricant. The green compacts were heated at 950 °C in an inert environment (Argon) at a rate of 5 °C per minute for 6 hours before being cooled in the furnace [21].

These are the stages found in sintering samples (Figure 1):

1. Rating increase of 5 °C per minute during heating from ambient to 500 °C.
2. Requiring a 500-degree °C (1 hour) soak time.
3. Rating increases by 5 °C/min when heating from 500 to 950 °C.
4. Six hours in a 950 °C water bath.
5. In a furnace with a constant flow of Argon, the temperature is lowered gradually to room temperature.

Table 2: Chemical composition of the prepared alloys (Wt%)

Specimen	Mg	Al	Si	Ca	Ti	Mn	Fe	O	Mo	Y
Zero-Alloy (85Ti-15Mo)	0.08	0.09	0.32	0.24	84.40	0.07	0.11	0.35	14.35	0.00
A-Alloy (84.5Ti-15Mo-0.5Y)	0.07	0.10	0.09	0.30	83.95	0.01	0.18	0.32	14.53	0.45
B-Alloy (84Ti-15Mo-1Y)	0.09	0.09	0.07	0.20	83.62	0.06	0.12	0.28	14.56	0.92
C-Alloy (83.5Ti-15Mo1.5Y)	0.09	0.10	0.04	0.30	82.93	0.05	0.18	0.23	14.68	1.37

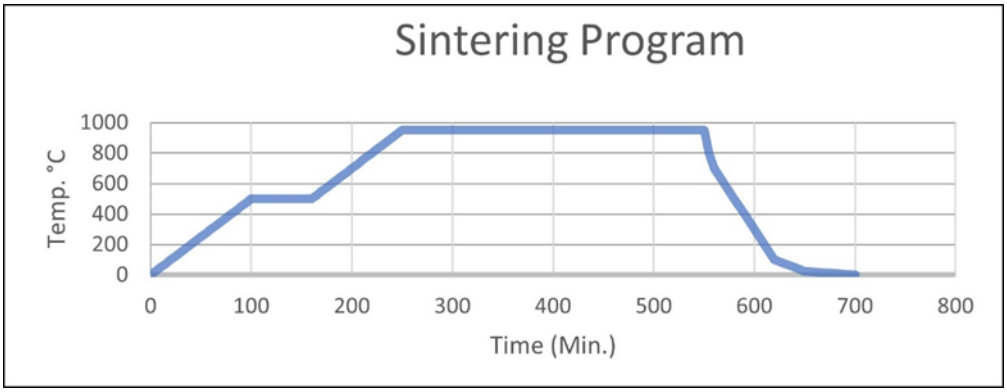

Figure 1: Heating cycle in sintering

Nitrogen, hydrogen, and oxygen were removed from the sintering atmosphere to prevent the composite from reacting unnecessarily. Table 2 lists four samples made with all of the powders used to make Ti-15Mo-xY and its composites.

Characterization of the prepared specimens

The X-ray diffraction (XRD) analysis was utilized to determine the crystal structures and phases present in the generated specimen (Shimadzu XRD-60000 X-Ray diffractometer). The radiation parameters were 20°-80° 2, 40 kV, 30 mA, and Cu K (=1.5409 A). Wet grinding with grades of (600), (800), (1000), and (2000), as well as polishing with diamond paste (1 m particle size), were employed to prepare the specimens for microstructure examination using a light optical microscope (Olympus/542037.Japan) and SEM type (CARL ZEISS ULTRA PLUS GEMINI FESEM). A solution of "10 g $FeCl^{3+}$ 25 mL HCL+100 mL distilled water" [22] was used to etch the specimens. The X-ray diffraction (XRD) was used to determine the phases and crystal structures of the specimen before and after yttrium was introduced (Shimadzu XRD-60000 X-Ray diffractometer). Devices for measuring Brinell hardness (Digitals Micro Brinell Hardness Tester TH 717) with an ASTM-required load of 187.5 KP for 10 s. (E10-15). The sintered samples can be analyzed for porosity using the standards set out in ASTM B327. The compressive testing was performed with a standardized, electronic universal testing machine under computer control (WDW-200KN).

Analysis of variance

The statistical method known as variance analysis (ANOVA) can be used to identify discrepancies in the means of communication between different groups in an experiment. When there are multiple experimental groups for a given independent (categorical) variable, analysis of variance (ANOVA) becomes warranted. The ANOVA terminology for independent variables is "factors," and the aggregations inside "factors" are "levels." Using a computerized analysis of variance (ANOVA) approach, researchers can determine how much variation in an experiment's response can be attributed to changes in individual parameters. Using analysis of variance, the effect of each input parameter on the machining process can be determined. The influence of yttrium addition on the properties of Ti-15Mo alloy is examined using the SPSS 26 statistical tool.

Results and Discussion

X-Ray diffraction analysis (XRD)

The powder of titanium, molybdenum, yttrium, and their alloys were X-ray diffraction analyzed to better understand their microscopic structure (Ti-15Mo, Ti-15Mo-XY). The XRD results for Ti-15Mo alloy with and without yttrium addition are displayed in Figure 2. The structure of Ti-15Mo-xY alloy sintered at 950°C is characterized by the formation of -Ti, Y, Y_2O_3, MO_3, and TiO_2 phases, as indicated by the indexing of standard cards representing JCPDS-ICDD 44-1288 and 29-1360. This finding is congruent with Wang *et al.* [13], who established that Mo and Y are necessary β -phase stabilizers.

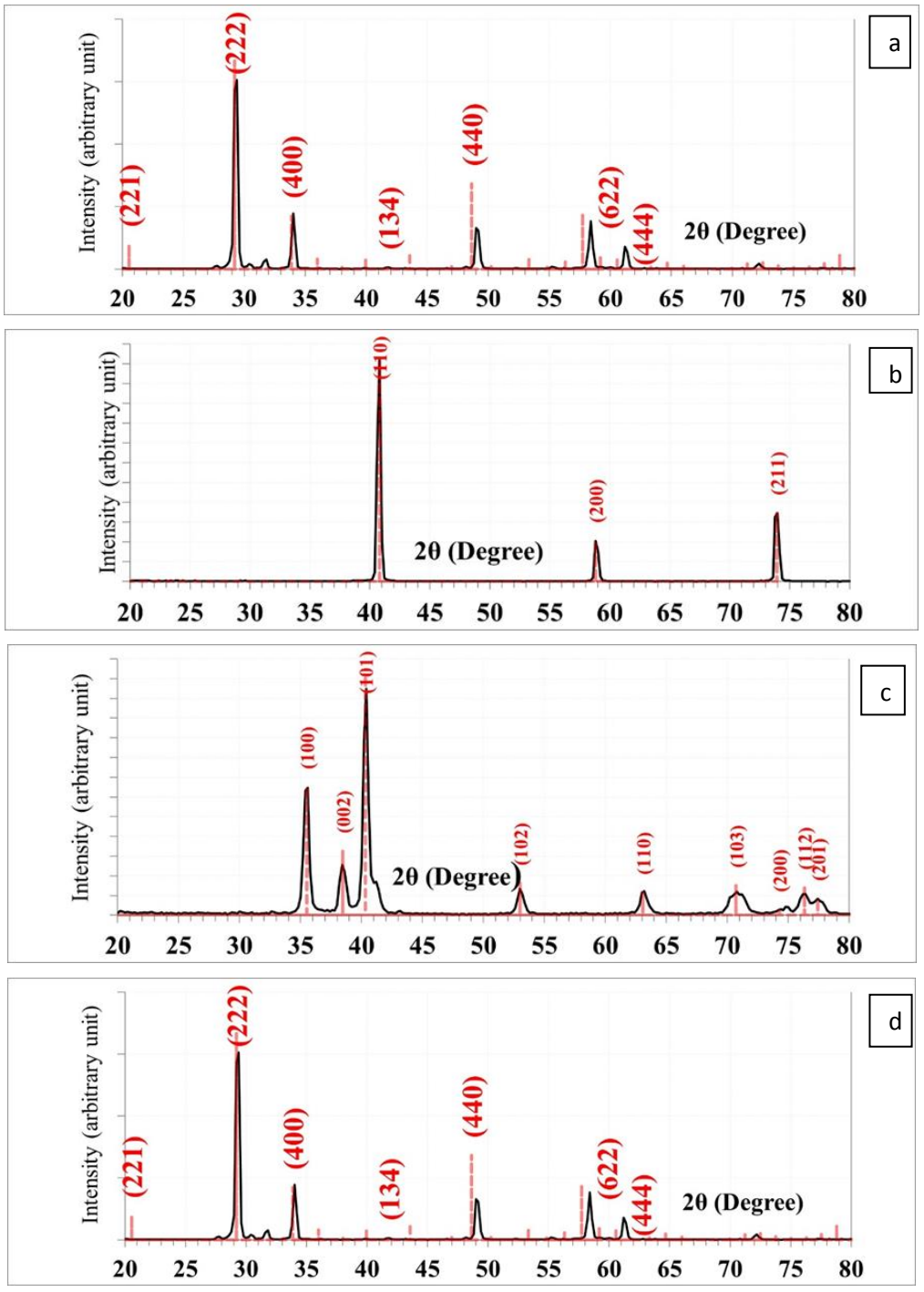

Figure 2: a) X-ray diffraction analysis for; Ti-15Mo, Ti-15Mo-0.5Y, Ti-15Mo-1.0 Y, and Ti-15Mo-1.5Y alloys, b) X-ray diffraction analysis for Mo powder, c) X-ray diffraction analysis for Ti powder, and d) X-ray diffraction analysis for Y element powder

Microstructure characterization for sintering alloys

The yttrium atoms were effective at refining the grains by segregating or precipitating at the grain boundaries in the optical microscope images of the microstructures of the new alloy after the addition of the yttrium element to the base metal. This can be seen clearly in 1.5 percent yttrium more than others because yttrium's ability to refine grains increases with increased yttrium content and this finding is in agreement with Zhang *et al.* [23]. The XRD test verified that the alloy's matrix is β phase. It was seen that the grain of β-Ti-15Mo became smaller and the microstructure was refined with the rise of Y concentration [24]. Yttrium additions will be at grain borders and refine-phase grains, as depicted in Figure 3A, B, C, and D.

The morphologies of both alloys are not equiaxed structures according to SEM. However, it is demonstrated that yttrium refines the equiaxed grains by segregating the grains and making the granules finer. The SEM images of Ti-Mo-xY revealed that Ti-Mo concurred with Won *et al.* [25] that precipitates along grain boundaries significantly increase.

Due to the high sensitivity of SEM images to the chemical composition, sintered samples exhibit a multiphase structure, with the β-Ti phase supporting the XRD findings. The grain boundaries and pores in the etched alloys were visible in the SEM images of various sizes. Figures 4A, 4B, 4C, and 4D displayed the SEM images of 4C and Zero alloys at various magnifications. Since a more uniform oxide film is more likely to form on small-grained microstructures in the passivated metals due to a more refined grain boundary distribution and triple junctions, the Ti-Mo-xY alloys exhibit an element of yttrium that is more uniform, well-distributed, and homogenous yttrium element. This is because of the good mixing and sintering temperature. Accordingly, Gollapudi [26] is correct.

The physical and mechanical properties

Porosity

Only a few larger pores or pore clusters are visible in alloys with an addition of about 0.5 percent in the Ti-Mo specimens with the addition of fine yttrium powder (Figure 5). However, as the yttrium content increases, the sizes of these pores increase, leading to an increase in porosity. The porosity test result was confirmed by the results from the optical light microscope, and it agrees with Khilfa [19].

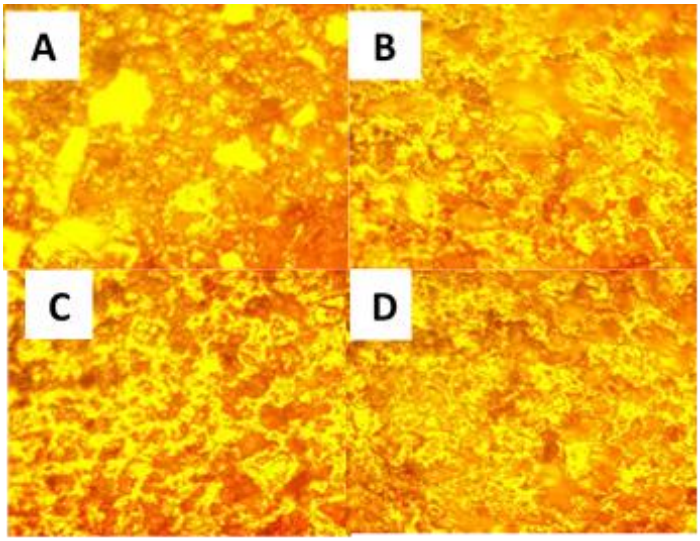

Figure 3: Microstructure for A) Ti-15Mo, B) A (Ti-15Mo-0.5Y) alloys, C) B (Ti-15Mo-1.0Y) alloys, and D) C (Ti-15Mo-1.5Y) alloys after sintering and etching (100 x)

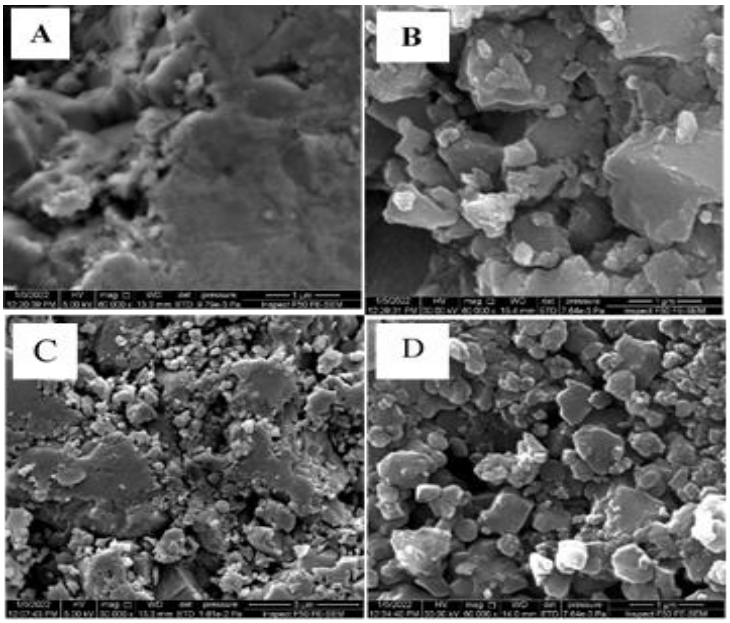

Figure 4: SEM images for etched; A) Zero (Ti-15Mo) alloy, B) A (0.5% Y) alloy, C) B (1.0%) alloy, and D) C (1.5% Y) alloy

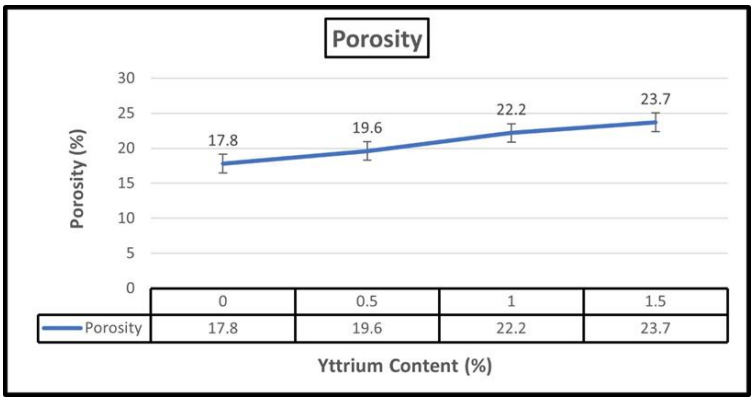

Figure 5: Change in the porosity after the yttrium addition

Using finer yttrium powder results in a little lower increase in porosity, which is in agreement with Limberg & Ebelb's [27] findings. Yttrium has a coefficient of thermal expansion (CTE) that is about greater than Titanium. Due to a noticeable thermal shrinkage, a somewhat large CTE mismatch could cause disintegration and the creation of porosity during cooling following extrusion.

The titanium alloy without the yttrium addition exhibits density more than it does with the addition because the yttrium generates porosity, which leads to a less compacted alloy, which results in a loss in density. This is due to the uneven form of the colony borders.

Table 3 provides the descriptive statistics for surface porosity for the four groups, with group Zero having the lowest mean value (17.8%) and group C alloy having the greatest mean value (23.7 percent).

The POST HOC test was employed for multiple comparisons between each pair of study groups since results in Table 4 for the test of homogeneity of variances (Levene's Statistic) indicate that the P-value was greater than 0.01 and that the data were normally distributed throughout the groups.

There was a highly significant difference between the groups, according to the ANOVA test reported in Table 5, P=0.01 at 3 degrees of freedom.

Table 3: Descriptive statistic for the porosity test

Porosity							
Alloys	N	Mean	Std. Deviation	Std. Error	95% Confidence Interval for Mean		Minimum	Maximum
					Lower Bound	Upper Bound		
A-Alloy	5	19.60	1.48	.66	17.75	21.44	17.80	21.50
B- Alloy	5	22.20	1.58	.707	20.23	24.16	20.50	24.30
C- Alloy	5	23.70	1.42	.635	21.93	25.46	21.40	25.10
Zero - Alloy	5	17.80	1.43	.64	16.02	19.57	16.10	19.50

Table 4: Homogeneity of Variances for porosity test

Levene Statistic	df 1	df 2	Sig.
.220	3	16	.881

Table 5: ANOVA for porosity test

	Sum of Squares	df	Mean Square	F	Sig.
Between Groups	104.038	3	34.679	15.808	.000
Within Groups	35.100	16	2.194		

The hardness of specimens (Zero alloy and Ti-15Mo-xY with different concentrations) was compared using the multiple comparison test (POST HOC TEST), and all results showed that the hardness of the C alloy group was higher than that of the other groups with a highly significant difference and the large variability or difference found in the 1.5 Y concentration, as exhibited in Table 6.

Hardness measurements

Table 4 shows the graph of Brinell's hardness values for the β-type Ti-Mo-xY alloy (x = 0.5, 1.0, and 1.5 wt. percent) biomedical alloys (Figure 6). It can be seen that the hardness values of the β-type Ti-Mo-xY alloy biomedical alloys vary when Y is added. The hardness of Ti-Mo alloy is (341.65HB), and the yttrium addition improved the hardness and the hardness value as the yttrium percentage rose. The hardness of the A, B, and C alloys, which are illustrated in Figure 6, are 405.33, 435.76, and 510.05, respectively.

Table 6: Post Hoc test /multiple comparisons for porosity

Dependent Variable: Porosity Dunnett t (2-sided)						
(I) GROUPS	(J) GROUPS	Mean Difference (I-J)	Std. Error	Sig.	95% Confidence Interval	
					Lower Bound	Upper Bound
A- Alloy	Zero-Alloy	C 1.8	.93	.172	.6284	4.2284
B- Alloy	Zero-Alloy	B 4.40[a]	.93	.001	1.9716	6.8284
C- Alloy	Zero-Alloy	A 5.90[a]	.93	.000	3.4716	8.3284

[a]The mean difference is significant at the 0.05 level

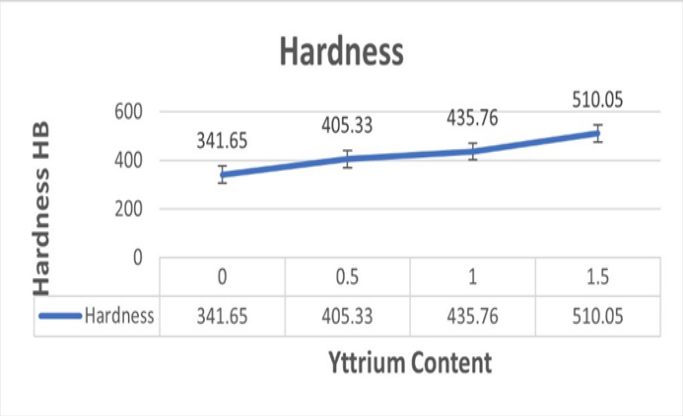

Figure 6: Change in hardness after the addition of yttrium

In a traditional casting technique, oxygen diffuses quickly through the liquid melt, making it simple for yttrium oxide to develop through a liquid-solid interface interaction. Another practical method of obtaining yttrium oxide is through the decomposition of supersaturated solid solutions of the rare earth element in the matrix. However, yttrium will scavenge oxygen from the matrix during the sintering process at solid-solid interfaces under the control of the interfacial kinetics. Therefore, the absence of sufficient oxygen in the environment prevents the yttrium-rich particles from producing enough Y2O3. On the other hand, Y-Ti-O solid solution may develop because at the sintering temperature Ti is soluble in yttrium.

According to a prior work by Court *et al.* (1988), only nonstoichiometric lanthanum oxides can occur during the annealing process of rapidly solidified Ti-La alloy by oxidizing metallic lanthanum precipitated during the rapidly solidified processing [28]. This shows that the internal oxidation of rare earth elementals in a solid-state process can produce rare earth-rich particles more easily than stoichiometric rare earth oxides. The only way for Y to scavenge more oxygen from the matrix and generate oxides is if the Y-rich particle-matrix interface is destroyed and a new interface is created.

Furthermore, Naka *et al.* (2010) noted that Y_2O_3 can dissolve and reprecipitate as a result of the shifting of grain boundaries. Moreover, it has been demonstrated that the moving grain boundary can draw solute from the matrix and boost local solute concentrations [29].

Both alloys became denser, which greatly improved their strength. However, the yttrium oxides in the Ti-Mo alloy with yttrium addition were formed as a result of the continued disintegration of the Y-rich particles, sufficient diffusion, and reactivity between Y and O in the surrounding environment [30].

The oxides, which are harder than the matrix and will reinforce the Ti alloy by preventing dislocation movement and crack growth, will increase the strength of the Ti-Mo-Y alloy. Likewise, as a result of the creation of oxides continuing to consume oxygen from the matrix, the Ti-Mo-xY alloy strengthened by greater yttrium addition can have better hardness and compressive strength due to the production of yttrium oxides in the matrix.

Table 7 indicates the descriptive statistics for surface hardness for the four groups, with group Zero having the lowest mean value (341.65 HB) and group C alloy having the greatest mean value (510.05 HB).

The POST HOC test was employed for multiple comparisons between study groups since the results in Table 8 for the test of homogeneity of variances (Levene's Statistic) indicate that the P-value was more than 0.01 and that the data were normally distributed throughout the groups.

ANOVA test seen in Table 9 reveals that there was a highly significant difference among the groups P≤ 0.01 at 3 degrees of freedom.

Table 7: Descriptive statistic for hardness test

Hardness								
Alloys	N	Mean	Std. Deviation	Std. Error	95% Confidence Interval for Mean		Minimum	Maximum
					Lower Bound	Upper Bound		
A-Alloy	6	405.33	6.28	2.56	398.74	411.92	397.20	412.50
B- Alloy	6	435.77	2.76	1.13	432.87	438.66	432.40	439.40
C- Alloy	6	510.05	3.37	1.37	506.52	513.58	505.70	515.00
Zero -Alloy	6	341.65	6.08	2.48	335.27	348.03	332.30	350.90

Table 8: Test of homogeneity of variances for hardness test

Test of homogeneity of variances for hardness			
Levene Statistic	df 1	df 2	Sig.
1.447	3	20	.259

Table 9: ANOVA for Hardness test

	Sum of Squares	df	Mean Square	F	Sig.
Between Groups	88022.783	3	29340.928	1231.269	.000
Within Groups	476.597	20	23.830		

Table 10: Post Hoc test /multiple comparisons for hardness test

Dependent Variable: Hardness Dunnett t (2-sided)						
(I) GROUPS	(J) GROUPS	Mean Difference (I-J)	Std. Error	Sig.	95% Confidence Interval	
					Lower Bound	Upper Bound
A- Alloy	Zero-Alloy	C 63.68[a]	2.82	0.000	56.52	70.84
B- Alloy	Zero-Alloy	B 94.12[a]	2.82	0.000	86.96	101.28
C- Alloy	Zero-Alloy	A 168.40[a]	2.82	0.000	161.24	175.56

[a]The mean difference is significant at the 0.05 level

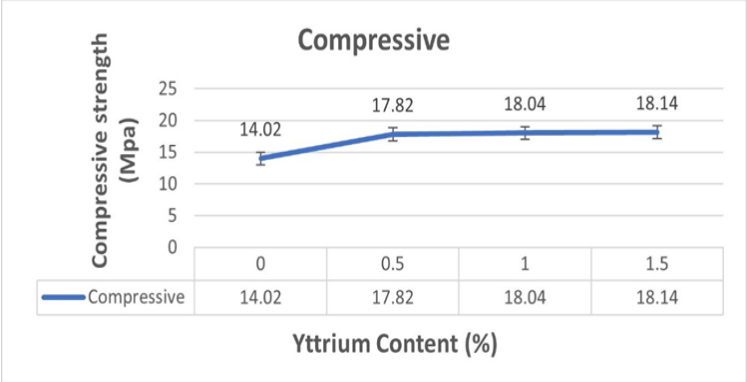

Figure 7: Change in compressive strength after the addition of yttrium

The hardness of specimens (Zero alloy and Ti-15Mo-xY with different concentrations) was compared using the multiple comparison test (POST HOC TEST), and all results showed that the

hardness of the C alloy group was higher than that of the other groups with a highly significant difference and the large variability or difference found in the 1.5 Y concentration, as demonstrated in Table 10.

Compression test

The compressive strength of Ti-Mo alloy is improved when yttrium is introduced. When yttrium is added to titanium alloy in elemental form, some of which dissolves into the molten alloy and some reacts with oxygen from titanium powders or/and the atmosphere to form Y_2O_3 particles, which is confirmed by the XRD result showing Y_2O_3 formation. The C (Ti-Mo-1.5Y) alloy has the highest compressive strength value among the other alloys, as can be displayed in Figure 7. Therefore, it would be reasonable to predict that preventing dislocation movement across Y_2O_3 phases in alloys employing a dispersion mechanism would improve the mechanical properties of the alloy. The strong particles may prevent the dislocations from sliding, and more dislocations gather close to the Y_2O_3 particles. As a result, because Y_2O_3 particles are stronger than the matrix, substantially more applied tension is placed on them. As a result, the addition of Y_2O_3 particles increased the compressive strength, with the improvement depending on the yttrium percentage of the alloy.

The POST HOC test was employed for multiple comparisons between study groups since the test of homogeneity of variances (Levene's statistic) in Table 12 indicates that the P-value was greater than 0.01 and that the data were normally distributed throughout the groups.

There was a highly significant difference between the groups, as shown by the ANOVA test presented in Table 13, P=0.01 at 3 degrees of freedom.

The hardness of specimens (Zero alloy and Ti-15Mo-xY with different concentrations) was compared using the multiple comparison test (POST HOC TEST) as shown in Table 14, and all results showed that the hardness of the C alloy group was higher than that of the other groups, with a highly significant difference and the large variability or difference found in the 1.5 Y concentration.

Table 11: Descriptive statistic for compressive test

Compressive								
Alloys	N	Mean	Std. Deviation	Std. Error	95% Confidence Interval for Mean		Minimum	Maximum
					Lower Bound	Upper Bound		
A-Alloy	5	17.82	1.087	.48621	16.47	19.16	16.30	19.20
B- Alloy	5	18.04	.991	.44340	16.80	19.27	16.70	19.20
C- Alloy	5	18.14	.867	.38807	17.06	19.2	17.20	19.40
Zero - Alloy	5	14.02	1.0	.48104	12.68	15.35	12.50	15.20

Table 12: Homogeneity of variances for compressive test

Levene Statistic	df 1	df 2	Sig.
.141	3	16	.934

Table 13: ANOVA for comparisons test

	Sum of Squares	d.f	Mean Square	F	Sig.
Between Groups	59.669	3	19.890	19.524	.000
Within Groups	16.300	16	1.019		

Table 14: Post Hoc test /multiple comparisons for comparisons test

Dependent Variable: Comparisons Dunnett t (2-sided)						
(I) GROUPS	(J) GROUPS	Mean Difference (I-J)	Std. Error	Sig.	95% Confidence Interval	
					Lower Bound	Upper Bound
A- Alloy	Zero-Alloy	3.8[a]	.63	.000	2.14	5.45
B- Alloy	Zero-Alloy	4.02[a]	.63	.000	2.36	5.67
C- Alloy	Zero-Alloy	4.12[a]	.63	.000	2.46	5.77

[a]The mean difference is significant at the 0.05 level

Conclusion

Yttrium addition to Ti-15Mo alloy was fabricated through the powder metallurgy technique and was investigated for porosity, compressive strength, and hardness. The experimental investigations were carried out through the tests and the following conclusions are acquired.

1. It is observed that the increase in porosity percent of the manufactured alloys with 0.5, 1.0, and 1.5 wt. % of Y in comparison to the Ti-15Mo due to the addition of yttrium in the matrix phase.
2. It is observed that an increase in the compressive strength and hardness of alloys made with 0.5, 1.0, and 1.5 wt. % of Y as compared with Ti-15Mo due to the effect of yttrium addition into the matrix phase.

Acknowledgments

The authors would like to thank the University of Baghdad and College of Dentistry and the Department of Metallurgical Engineering, Materials Engineering Faculty, University of Babylon, Hillah, Iraq /Iraq for their support.

Funding

This research did not receive any specific grant from funding agencies in the public, commercial, or not-for-profit sectors.

Authors' contributions

All authors contributed to data analysis, drafting, and revising of the paper and agreed to be responsible for all the aspects of this work.

Conflict of Interest

The authors have no conflicts of interest relevant to this article.

References

[1]. Oshida Y., Tuna E.B., Aktören O., Gençay K., Dental implant systems, *International Journal of Molecular Sciences*, 2010, **11**:1580 [Crossref], [Google Scholar], [Publisher]

[2]. de Viteri V.S., Fuentes E., 'Titanium and Titanium Alloys as Biomaterials', in J. Gegner (ed.), Tribology - Fundamentals and Advancements, IntechOpen, London, 2013, 10.5772/55860 [Crossref], [Google Scholar], [Publisher]

[3]. El-Hajje A., Kolos E.C., Wang J.K., Maleksaeedi S., He Z., Wiria F.E., Choong C., Ruys A.J., Physical and mechanical characterization of 3D-printed porous titanium for biomedical applications, *Journal of materials science. Materials in medicine*, 2014, **25**:2471 [Crossref], [Google Scholar], [Publisher]

[4]. Abdel-Hady Gepreel M., Niinomi M., Biocompatibility of Ti-alloys for long-term implantation, *Journal of the mechanical behavior of biomedical materials*, 2013, **20**:407 [Crossref], [Google Scholar], [Publisher]

5.

[6]. Guimarães Z., Damatta R.A., Guimarães R.S., Filgueira M., A Novel Porous Diamond - Titanium Biomaterial: Structure, Microstructure, Physico-Mechanical Properties and Biocompatibility, *Anais da Academia Brasileira de Ciências*, 2017, **89**:3111 [Crossref], [Google Scholar], [Publisher]

[7]. Al-Humairi A.N.S., Majdi H.S., Al-Humairi S.N.S., Al-Maamori M., *BIOMATERIALS: Multidisciplinary approaches and their related applications*. White Falcon Publishing, 2020 [Google Scholar], [Publisher]

[8]. Xu D.S., Wang H., Zhang J.H., Bai C.G., Yang R., Titanium alloys: from properties prediction to

performance optimization. In: Andreoni W, Yip S (eds) Handbook of materials modeling, Springer, Cham, 2020 [Crossref], [Google Scholar], [Publisher]
[9]. Kolli R.P., Devaraj A., A review of metastable beta titanium alloys, *Metals*, 2018, **8**:506 [Crossref], [Google Scholar], [Publisher]
[10]. Soundararajan S.R., Vishnu J., Manivasagam G., Muktinutalapati N.R., Heat treatment of metastable beta titanium alloys, In *Welding-Modern Topics*, IntechOpen, 2020 [Crossref], [Google Scholar], [Publisher]
[11]. Hassan A.G., Yajid M.M., Saud S.N., Bakar T.A., Arshad A., Mazlan N., Effects of varying electrodeposition voltages on surface morphology and corrosion behavior of multi-walled carbon nanotube coated on porous Ti-30 at.%-Ta shape memory alloys, *Surface and Coatings Technology*, 2020, **401**:126257 [Crossref], [Google Scholar], [Publisher]
[12]. Mulyadi I.H., Arif Z., Nuswantoro N.F., Affi J., Niinomi M., Effect of particle size on adhesion strength of bovine hydroxyapatite layer on Ti-12Cr coated by using electrophoretic deposition (EPD) method, *IOP Conference Series: Materials Science and Engineering*, 2021, **1041**:012054 [Crossref], [Google Scholar], [Publisher]
[13]. Fajri H., Ramadhan F., Nuswantoro N.F., Juliadmi D., Tjong D.H., Manjas M., Affi J., Yetri Y., Electrophoretic deposition (EPD) of natural hydroxyapatite coatings on titanium Ti-29Nb-13Ta-4.6 Zr substrates for implant material. In *Materials Science Forum*, 2020, **1000**:123 [Crossref], [Google Scholar], [Publisher]
[14]. Wang Z.M., Ma Y.T., Zhang J., Hou W.L., Chang X.C., Wang J.Q., Influence of yttrium as a minority alloying element on the corrosion behavior in Fe-based bulk metallic glasses, *Electrochimica acta,* 2008, **54**:261 [Crossref], [Google Scholar], [Publisher]
[15]. Xu Z., Wang Y., Xu R., Hu Q., Shi D., Lu X., Research on microstructure and properties of Ti-15Mo-3Al alloy with high oxygen content, *Materials Research Express*, 2020, **7**:116528 [Crossref], [Google Scholar], [Publisher]
[16]. Bahador A., Hamzah E., Kondoh K., ABUBAKAR T.A., Yusof F., Umeda J., IBRAHIM M.K., Microstructure and superelastic properties of free forged Ti–Ni shape-memory alloy, *Transactions of Nonferrous Metals Society of China*, 2018, **28**:502 [Crossref], [Google Scholar], [Publisher]
[17]. Han M.K., Im J.B., Hwang M.J., Kim B.J., Kim H.Y., Park Y.J., Effect of indium content on the microstructure, mechanical properties and corrosion behavior of titanium alloys," Metals, 2015, **5**:850 [Crossref], [Google Scholar], [Publisher]
[18]. Ho W.F., Wu S.C., Hsu S.K., Li Y.C., Hsu H.C., Effects of molybdenum content on the structure and mechanical properties of as-cast Ti–10Zr-based alloys for biomedical applications, *Materials Science and Engineering: C*, 2012, **32**:517 [Crossref], [Google Scholar], [Publisher]
[19]. Hansen D.C., Metal corrosion in the human body: the ultimate bio-corrosion scenario, *The Electrochemical Society Interface*, 2008, **17**:31 [Google Scholar], [Publisher]
[20]. Khilfa A.H., *Effect of Y and Ge addition on Mechanical properties and Corrosion Behavior of Biomedical C℃ rMoAlloy (F75)*, (Doctoral dissertation, master thesis, Materials engineering, University of Babylon), 2015 [Google Scholar]
[21]. Ramaswamy R., Selvam B., Marimuthu P., Natarajan E., Influence of Yttrium Oxide Nano-particles in Ti6Al4V Matrix on Compressive and Hardness behavior, *International Journal of Mechanical Engineering and Technology*, 2018, **9**:1140 [Google Scholar], [Publisher]
[22]. Al-Murshdy J.M.S., Al-Deen H.H.J., Hussein S.R., "Investigation of the Effect of Indium Addition on the Mechanical and Electrochemical Properties of the Ti–15Mo Biomedical Alloy "Journal of Bio- and Tribo-Corrosion 2021, **7**:148 [Crossref], [Google Scholar], [Publisher]
[23] Lide D.R., (Ed.). *CRC handbook of chemistry and physics*, CRC press, 2004, **85** [Google Scholar], [Publisher]
[24]. Zhang D., Qiu D., Gibson M.A., Zheng Y., Fraser H.L., Prasad A., StJohn D., Easton M.A., Refining prior-β grains of Ti–6Al–4V alloy through yttrium addition, *Journal of Alloys and Compounds*, 2020, **841**:155733 [Crossref], [Google Scholar], [Publisher]
[25]. Fontana and Green, 1978, Corrosion Engineering, McGrow – Hill Book Company

[26]. Won S., Seo B., Park H.K., Kim H.K., Kang H.S., Park K., Impact of Yttrium on corrosion properties of titanium as a grain refiner, *Materials Today Communications*, 2021, **25**:101900 [Crossref], [Google Scholar], [Publisher].

[27]. Gollapudi S., Grain size distribution effects on the corrosion behaviour of materials, *Corrosion Science*, 2012, **62**:90 [Crossref], [Google Scholar], [Publisher].

[28]. Limberg W., Ebel T., Metal injection moulding of Ti-6Al-4V with yttrium addition, In *Key Engineering Materials*, 2016, **704**:20 [Crossref], [Google Scholar], [Publisher]

[29]. Court S.A., Sears J.W., Loretto M.H., Fraser H.L., The effect of liquid phase separation on the microstructure of rapidly solidified titanium-Rare earth alloys, *Materials Science and Engineering*, 1988, **98**:243 [Crossref], [Google Scholar], [Publisher]

[30]. Naka, S.; October, H.; Bouchaud, E.; Khan, T. Reprecipitation observed in Y2O3 dispersed titanium during heat treatment after cold rolling, Scripta Metallurgica 1989, **23**:501 [Crossref], [Google Scholar], [Publisher]

HOW TO CITE THIS ARTICLE

Yas Mohammed Musadaq, Ghassan Abdul-Hamid Naji, Haydar H. J. Jamal Al‑Deen. Effect of Yttrium Addition on Mechanical and Physical Properties of Ti15Mo Alloy As an Implant Material. *J. Med. Chem. Sci*., 2023, 6(5) 986-999
https://doi.org/10.26655/JMCHEMSCI.2023.5.6
URL: http://www.jmchemsci.com/article_159349.html